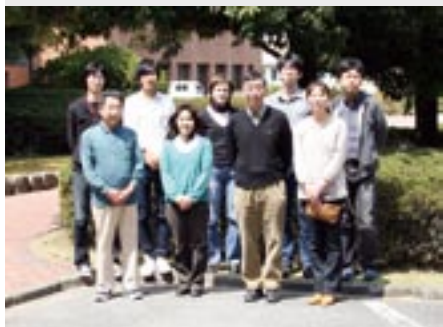


# Characterization of Magnetic Ultrathin Films by Novel Spectroscopic Methods

Department of Materials Molecular Science  
Division of Electronic Structure



YOKOYAMA, Toshihiko	Professor
NAKAGAWA, Takeshi	Assistant Professor
TAKAGI, Yasumasa	Assistant Professor
YAMAMOTO, Isamu	Post-Doctoral Fellow
ISAMI, Kyohei	Graduate Student
EGUCHI, Keitaro	Graduate Student
FUNAKI, Yumiko	Secretary
NOTO, Madomi	Secretary

Novel properties of magnetic metal ultrathin films have been attractive both from fundamental interest and from technological requirements. We are interested in drastic modification of metal thin films by surface chemical treatment such as adsorption-induced spin transitions and morphological changes. The magnetic properties are characterized by means of several kinds of spectroscopic methods like MOKE (Magneto-Optical Kerr Effect) using lasers and XMCD (X-ray Magnetic Circular Dichroism) using UV-visible lasers and XMCD (X-ray Magnetic Circular Dichroism) using synchrotron radiation soft X-rays.

Moreover, we have been exploiting new techniques based on UV photoemission magnetic circular dichroism (MCD) such as ultrafast time resolved UV MCD photoelectron emission microscopy (PEEM) for spatiotemporal magnetic imaging.

## 1. Observation of Two-Photon Photoemission Magnetic Circular Dichroism<sup>1)</sup>

In 2006, we discovered surprising enhancement of the UV-visible photoemission MCD from ultrathin Ni films on Cu(001) when the photon energy was tuned to the work function threshold.<sup>2)</sup> Based on this discovery, we succeeded in the first observation of UV MCD PEEM images of ultrathin magnetic films.<sup>3)</sup> This method allows us to perform in-laboratory MCD PEEM measurements instead of the usage of third-generation synchrotron radiation XMCD PEEM. Moreover, ultrafast UV MCD PEEM images were successfully obtained by using ultrashort pulsed lasers and a pump-and-probe technique.<sup>4)</sup>

Laser two-photon photoemission (2PPE) MCD should be also an attractive technique, because deeper valence bands can easily be detected without using vacuum UV light. In this work, we succeeded in the observation of significant enhancement in the 2PPE MCD near the work function threshold.

Figure 1(a) shows the MCD asymmetry of 12 monolayer (ML) Ni grown on Cu(001) as a function of excitation energy. An wavelength-tunable Ti:sapphire laser (80 MHz, 2.5 W, ~70

fs, 690–1050 nm) was employed in these measurements. The 4th-order harmonics for 1PPE (one-photon photoemission,  $h\nu = 5\text{--}6\text{ eV}$ ) and the 2nd-order for 2PPE ( $h\nu = 2.5\text{--}3\text{ eV}$ ). Noticeable enhancements of both the 1PPE and 2PPE MCD asymmetries are clearly observed in the vicinity of the work function threshold ( $\Phi = 5.15\text{ eV}$ ). It is noted that the spectral features of the 1PPE and 2PPE MCD resemble each other and that the negative maximum (~7%) in the 2PPE MCD is strong enough to apply this phenomenon to MCD PEEM measurements.

Figure 1(b) depicts the laser incidence angle ( $\theta$ ) dependence of the 1PPE and 2PPE MCD asymmetries from the same sample. In the 1PPE, the function is rather constant, although the MCD asymmetry should basically be proportional to  $\cos\theta$  ( $\theta$  corresponds to the angle between the magnetization and the light propagation direction). The deviation from the  $\cos\theta$  function is ascribed to the presence of the reflected light. Actually, the dashed line in Figure 1(b), which shows the calculated result using dielectric constants, agrees well with the observation. On the contrary, huge further enhancement is observed in the 2PPE at the grazing laser incidence ( $\sim 45^\circ$ ). The negative maximum reaches as much as ~28%. Since

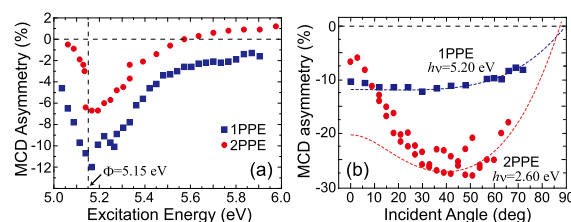


**Figure 1.** (a) 1PPE and 2PPE MCD asymmetries as a function of excitation energy ( $h\nu$  and  $2h\nu$  for 1PPE and  $2h\nu$ , respectively). The sample is perpendicularly magnetized Ni(12ML)/Cu(001) at room temperature and the laser incidence angle was  $0^\circ$  (normal incidence). Noticeable enhancements near the work function threshold (5.15 eV) can be seen as negative maxima. (b) Incidence angle dependence of 1PPE and 2PPE MCD asymmetries. 2PPE MCD shows negative maxima at  $\sim 45^\circ$  incidence. Dashed lines are the calculated results using a simple model.

PEEM experiments require grazing light incidence, the present finding is essentially important for the 2PPE MCD. The dashed line in Figure 1(b) again agrees fairly well with the observation. The calculation was done by assuming that only the first photon contributes to the MCD since the second photon excites the hot electron that is regarded as a free electron without spin-orbit coupling. Theoretical study is needed to understand the present observation in detail.

## 2. Structural and Magnetic Properties of Ultrathin Iron Nitride Epitaxial Films Grown on Cu(001)

Bulk iron nitrides exhibit various kinds of phases depending on the Fe/N stoichiometry, and many of the Fe-rich phases show ferromagnetism. It is interesting to investigate magnetic and structural properties of ultrathin iron nitride films. We have succeeded in the preparation of very flat ultrathin iron nitride films grown epitaxially on Cu(001) by the sequential process of depositing elemental Fe, subsequent  $N^+$  bombardment, and annealing at  $\sim 670$  K. Figures 2(a) and 2(b) show respectively the  $p4gm(2\times 2)$  LEED (low energy electron diffraction) pattern and the STM (scanning tunnel microscopy) image of the 1 ML  $Fe_2N$  film. The Fe/N stoichiometry of 2:1 was verified separately by the X-ray absorption spectra (XAS) intensity. A sharp LEED pattern in Figure 2(a) and a wide terrace observed in the STM image of Figure 2(b) confirm the extreme flatness of the film. The LEED  $I$ - $V$  curves were measured and analyzed to determine quantitative surface structures. The surface structure obtained is shown in Figure 2(c). The surface Fe atoms are squeezed due to embedding of the N atoms, leading to the  $p4gm(2\times 2)$  reconstructed surface.

By conducting a similar preparation procedure, a 2 ML iron nitride epitaxial film was also obtained. Interestingly, the Fe/N stoichiometry is found to be 4:1 by XAS, and the tensor LEED analysis has elucidated that the topmost layer structure is nearly identical to that of 1 ML  $Fe_2N$ , while the second layer contains only Fe, as seen in Figure 2(d). Such surface structures are found to mimic the bulk  $\gamma$ - $Fe_4N$  structure, where Fe forms *fcc* lattice with the N atom located at the center of the

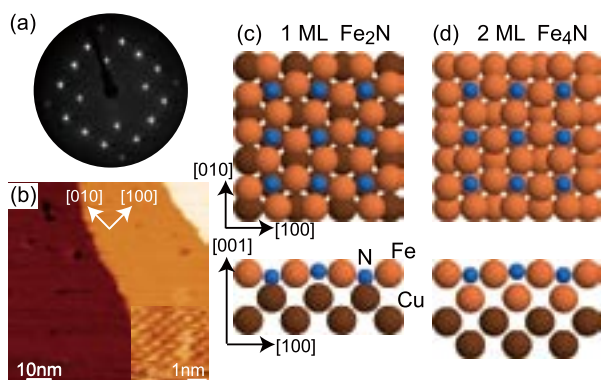


**Figure 2.** (a)  $p4gm(2\times 2)$  LEED pattern, (b) STM images, and (c) surface structure of the 1 ML  $Fe_2N$  film on Cu(001), and (d) that of the 2 ML  $Fe_4N$  film on Cu(001). The surface structure was determined quantitatively by the tensor LEED analysis.

lattice. By neglecting the occurrence of the  $p4gm(2\times 2)$  surface reconstruction, the 1 ML  $Fe_2N/Cu(001)$  structure can be regarded as one  $\gamma$ - $Fe_4N$  layer containing N, while the 2 ML  $Fe_4N$  structure corresponds to the unit cell of  $\gamma$ - $Fe_4N$ .

Magnetic properties were investigated by XMCD using the Beamline 4B of the UVSOR-II synchrotron radiation facility in IMS and our high-field & low-temperature XMCD apparatus recently developed.<sup>5)</sup> Figure 3(a) shows the angular dependent magnetization ( $M$ - $H$ ) curves of 1–4 ML iron nitride films on Cu(001). The  $M$ - $H$  curves along the  $\theta = 0^\circ$  direction imply that the surface normal is a magnetically hard axis, while the grazing angle ( $\theta = 55^\circ$ ) data indicates an easy axis within the film plane. The total magnetic moments  $m = m_{\text{spin}} + m_{\text{orb}}$  and the direction dependent orbital magnetic moments  $m_{\text{orb}}$  were obtained by the XMCD sum-rule analysis. The total magnetic moment  $m$  [Figure 3(a)] of 1 ML is rather small possibly due to the formation of strong chemical bonds between Fe and N. It increases with the thickness and seems to approach the bulk  $\gamma$ - $Fe_4N$  value of  $2.2 \mu_B$ . The orbital magnetic moment  $m_{\text{orb}}$  [Figure 3(b)] is always larger in the in-plane ( $\parallel$ ) direction than in the perpendicular ( $\perp$ ) direction. The difference between  $m_{\text{orb}}^{\parallel}$  and  $m_{\text{orb}}^{\perp}$  is  $\sim 0.06 \mu_B$ , which corresponds to the uniaxial magnetic anisotropy constant  $K_u$  of  $\sim 0.1$  meV/atom. This implies semiquantitative agreement in the present macroscopic and microscopic observations. The large in-plane magnetic anisotropy of the present system is resulted from a large anisotropy in the spin-orbit interaction.

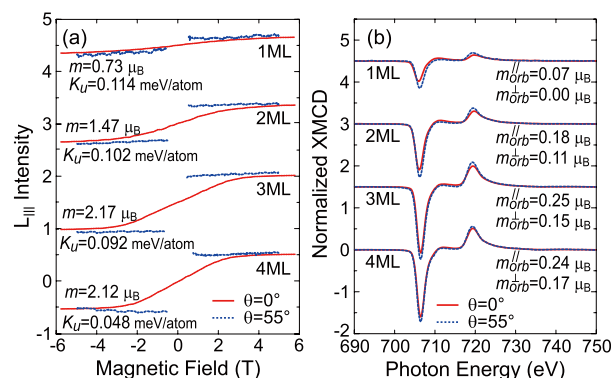


**Figure 3.** (a) Magnetization curves of 1–4 ML iron nitride films on Cu(001) at  $T = 5$  K, recorded by the Fe L3-edge circularly polarized X-ray absorption intensity and (b) the angle dependent XMCD spectra of the same samples at  $T = 5$  K and  $H = \pm 5$  T. The X-ray incident angles  $\theta = 0^\circ$  and  $55^\circ$  correspond respectively to normal and grazing magnetization measurements.

## References

- 1) T. Nakagawa, I. Yamamoto, Y. Takagi, K. Watanabe, Y. Matsumoto and T. Yokoyama, *Phys. Rev. B* **79**, 172404 (2009).
- 2) T. Nakagawa and T. Yokoyama, *Phys. Rev. Lett.* **96**, 237402 (2006).
- 3) T. Nakagawa, T. Yokoyama, M. Hosaka and M. Katoh, *Rev. Sci. Instrum.* **78**, 023907 (2007).
- 4) T. Nakagawa, K. Watanabe, Y. Matsumoto and T. Yokoyama, *J. Phys.: Condens. Matter* **21**, 314010 (2009).
- 5) T. Nakagawa, Y. Takagi, Y. Matsumoto and T. Yokoyama, *Jpn. J. Appl. Phys.* **47**, 2132 (2008).